Semiannual Technical Report,
1 November 1960 - 30 April 1961

CONDENSER HEAT REJECTION SYSTEMS

Prepared for

Technical Director
Office of Space Flight Programs
National Aeronautics and Space Administration

(NASA Contract No. NAS 7-11)

(NASA CR-55715;

EOS Report 1588-2Q-1)

30 April 1961 66 p refs

Prepared by

Lance Hays

Lance Hays and
Project Supervisor

Arthur Widawsky

Arthur Widawsky
Engineer

Approved by

J. Neustein

J. Neustein, Manager
ADVANCED POWER SYSTEMS
DIVISION

0845461

ELECTRO-OPTICAL SYSTEMS, INC., PASADENA, CALIFORNIA

TABLE OF CONTENTS

LIST OF ILLUSTRATIONS

LIST OF TABLES

1. SUMMARY

This report presents a summary of the technical effort and major results for the first six months of an investigation of condensers applicable to space power systems employing Rankine cycles. In spite of recent interest in this subject* adequate data describing the hydrodynamic and heat transfer characteristics of such components are lacking. An experimental investigation was initiated at EOS to supply this design data for several condenser techniques using water and mercury as test fluids (Ref. 1). However, the range of flow and geometric variables tested are limited. The present program is an extension of this earlier effort and is devoted to the further investigation of direct and spray condensers.

The prime areas of interest for spray condensers were:

1. Extension of the range of flow variables tested for constant area units.
2. A study of the time history of interface formation.
3. A study of simplification of the injector design.
4. A study of the use of variable area mixing chambers to increase stability and pressure rise.
5. Investigation of manifolded spray tubes.
6. Formulation of generalized design data and relationships which are given in terms of quantities applicable to power systems designs.

---

* A symposium sponsored by NASA was recently held at EOS (18 April 1961) for NASA contractors and others engaged in studies of condensing mercury. The following organizations which are engaged in this field sent representatives.

AEC	Electro-Optical Systems	WADD
Aerojet General	NASA	
Atomics International	Tapco	

Each organization's contributions to this meeting are presently being summarized and will be submitted individually to NASA.

7. Preliminary designs for typical power systems or applications.
8. Investigation of scaling problems associated with condensers.

For direct condensers technical effort was directed toward:

1. Extension of direct condenser investigations to a wider range of variables.
2. An investigation of the operating limits of various types of direct condensers.
3. A study of available pressure drop correlation methods.

The experimental portions of the first six months of the program were conducted on an existing mercury test loop. Testing of constant area spray condensers were conducted with a simplified injection technique (central injector). The range of variables was increased to the maximum possible within the capabilities of the existing test loop. A study of the time history of interface formation was made for these spray condensers with a high speed camera (Sec. 4).

Experimental investigations of transparent and metal direct condensers were conducted during this period. The range of flow and geometric variables were extended for the transparent test sections. Pressure drop measurements were made for isothermal two-phase mercury flow in the metal test section. Results were compared to those predicted by an existing pressure drop correlation (Sec. 2).

The major analytical effort on spray tubes was calculation of the theoretical maximum pressure rise for both constant and variable area spray tubes (Sec. 3). This analysis has been used to select spray tube geometries and test conditions for the second half of the program. Additional calculations were made to correlate spray tube data and compare pressure rise results to those predicted by the analysis.

Fabrication of a modified mercury test loop was also accomplished during the first half of the program (Sec. 5). This loop was required to further extend the range of flow and geometric variables. Increased capacity was also required to conduct multitube tests and to test vapor velocities corresponding to current power system designs. Vacuum capability was provided to enable the condensers to be tested at pressures which also correspond to the current power system designs.

The main areas to be investigated during the remainder of the test program include:

1. Testing of constant area spray condensers over the increased range of variables possible with the modified test loop.
2. Testing of variable area spray condensers and comparison of experimental results with those of the analysis and with experimental results for constant area geometries.
3. Development of generalized design data relationships for spray condensers which are expressed in terms of quantities applicable to power systems using the Rankine cycle.
4. Testing of a multitube spray condenser configuration to determine the feasibility of manifolding several units.
5. Preliminary designs for typical power systems and applications using (3) and (4).
6. Investigation of scaling problems for condensers and recommendations for testing.

2. DIRECT CONDENSER INVESTIGATIONS

2.1 Review of Direct Condenser Investigations with Mercury

Previous experimental investigations at EOS of direct condensers for mercury have consisted of two related efforts:

1. Tests conducted with transparent single tubes (horizontal) over a range of flow rates and geometries
2. Design and testing of an all-metal, multi-tube prototype radiator condenser

One of the most important problem areas examined in this work was determination of flow and geometric parameters which result in performance of the condenser with vapor-free flow at the outlet. Other forms of instability may be present in a condenser but this was felt to be the most important criterion of performance. The general results are in agreement with the findings of other investigators and have been discussed elsewhere (Ref. 2). Briefly, it was found that for all flow conditions tested, use of tube diameters less than about 0.16" resulted in slug-free flow at the condenser outlet. Larger tubes could not be operated with the above outlet condition for any flow rate and tube curvature tested.

It should be emphasized, however, that the failure of larger tubes to perform is due to the interaction of gravity with the flow process. No limitation of this type should exist for operation in a zero-gravity environment.

Pressure drop measurements were made for all test runs. However, a basic limitation exists for pressure drop measurements on tests of this type. For short test sections the pressure rise due to recovery of momentum of the condensing vapor may be about equal to the frictional pressure drop. As a result, the measured pressure drop is very low or negligible. For the proper combination

of flow and geometric conditions, the total pressure drop has even been measured to be positive. This possibility occurs if

$$\Delta p_f < \Delta p_{mom}$$

since 2-1

$$\Delta p_m = \Delta p_f - \Delta p_{mom}$$

where

Δp_m = measured pressure drop

Δp_f = frictional pressure drop

Δp_{mom} = pressure rise due to recovery of vapor momentum

Frictional pressure drop for this type of test must be deduced from measurements of flow rate, total pressure drop, and quality as shown by the following relations:

$$\Delta p_f = \Delta p_m + \Delta p_{mom} \qquad 2\text{-}2$$

and

$$\Delta p_{mom} = \frac{\rho_v V_v^2}{g} + \frac{\rho_L V_L^2}{g} - \frac{\rho_L V_F^2}{g} \qquad 2\text{-}3$$

$$= \frac{x_v^2 \dot{m}_t^2}{\rho_v A_t^2 g} + \frac{(1-x_v)^2 \dot{m}_t^2 s^2}{\rho_L A_t^2 g} \qquad 2\text{-}4$$

where

ρ_v = vapor density

ρ_L = liquid density

V_v = vapor velocity at inlet

V_L = liquid velocity at inlet (for $x_v < 1$)

x_v = vapor quality at inlet

$\dot{m}_t$ = total flow rate, measured at outlet

A_t = tube flow area

s = slip factor; $V_L = sV_v$

V_p = liquid velocity out of condenser

Any uncertainties in vapor quality, vapor-liquid slip (which is unknown), or liquid flow rate, directly affect the estimate of frictional pressure drop. With these uncertainties, frictional pressure drop for short test sections is difficult to establish accurately from experimental data.

For longer test sections the frictional pressure drop becomes larger than the momentum pressure rise but the same uncertainties are encountered in condensing flow. The prediction of pressure drop in condensing systems is currently being made by use of the Martinelli correlation (Ref. 3). The validity of this method, however, has yet to be satisfactorily established for mercury systems. Moreover, the measurement problem noted above introduces inaccuracies in the comparison of the predicted and measured pressure drops.

In view of these considerations a special test program was evolved to evaluate the Martinelli correlation (MC) for mercury. The test program consisted of the following steps:

1. Measurement of pressure drop in <u>isothermal flow</u> for a range of values of inlet vapor quality.
2. Measurement of pressure drop in <u>condensing flow</u> for a range of values of inlet and outlet vapor qualities.

The first step provides the isothermal conditions specified in the original MC, whereas the second step provides systematic deviations from the isothermal conditions. For the above program, the experimental technique and results obtained to date are described below.

If condensation in the test section in isothermal tests is limited to a small amount, a direct measure of the frictional pressure drop can be made and results can be compared directly with correlations such as that of Martinelli. For example, for the tests reported below, the maximum uncertainty in the pressure drop measurements due to vapor-liquid slip uncertainty and condensate pressure recovery was about 4 percent. Moreover, the results obtained in isothermal two-phase experiments should be directly applicable to condensing mercury with addition of the momentum term. For example, isothermal water data has been successfully applied to predict pressure drop in boiling and condensing steam-water systems. (Ref. 4)

2.2 Plan of Extended Investigation

Tests were conducted on the existing mercury test loop with a test section fabricated of stainless steel. Data was taken for essentially constant vapor Reynolds number (~ 8000). The relative amounts of liquid and vapor phases were varied by varying the inlet quality to the test section (by changing the upstream heat losses). In this manner data was obtained over a range of inlet quality from 1.0 to 0.515. The data obtained for quality equal to 1.0 corresponded to conditions for which accurate calculations could be made. Consequently, this data was used to establish the accuracy of the flow and pressure drop measurements. For comparison, all data were reduced to the factors used by Martinelli.

2.3 Description of Test Unit

The test section for isothermal pressure drop tests was constructed of stainless steel. Mercury flowed through a straight tube with a 0.157" i.d. Pressure taps were separated by distance of 16-1/4". The taps were .040" holes which were connected in a horizontal run of 1/8" tubing to condensate chambers and then to a mercury manometer. The purpose of the condensate chambers was to allow for level variations in the manometer and subsequent entry of vapor with the pressure tap leg, without inducing an error in the readings.

An outer jacket was welded to the test section in order to circulate cooling air. This jacket was instrumented to record the inlet and outlet air temperatures and air flow rate. Provision of a mixing section before the air outlet temperature resulted in a radial temperature gradient of less than 2°F. The jacket was heavily insulated to reduce the external heat loss.

With this instrumentation, the jacket was used as a calorimeter when cooling air was flowing. Measurement of the condensed mercury flow rate and application of a heat balance (cf. Sec. 2.4) gave a direct measure of vapor inlet quality and the upstream heat loss.

Temperatures were recorded with the aid of Chromel-Alumel thermocouples inserted into the flowing system. The mercury vapor temperature was recorded at the inlet and outlet of the test section for isothermal runs. For calorimeter runs the liquid temperature out replaced the outlet vapor temperature.

2.4 Test Procedure and Accuracy of Measurements

The test setup for isothermal pressure drop measurements is shown schematically in Fig. 2-1. The following sequence was used in order to obtain two-phase pressure drop data for comparison with that predicted by the criterion of Martinelli.

1. An interface was established in the calorimeter test section. (Fig. 2-1a) The presence of the interface inside the test section was confirmed by the outlet temperature measurement of the liquid mercury. The formation of a stable interface was assured by previous testing with a glass geometry identical to the metal one tested. Heat balance measurements were made on the cooling air and vapor in order to determine the quality of the vapor.

2. The cooling air was shut off. This resulted in movement of the vapor-liquid interface to the position shown in Fig. 2-1b. After sufficient elapse of time to establish thermal equilibrium, the pressure drop and vapor flow rate were recorded.

The vapor flow rates for (1) and (2) were approximately equal. The heat lost from the boiler to the test section was assumed to be equal for the two runs. The quality for (2) is then given by the following: (For runs with no superheat)

$$x_v = \frac{Q_1 - Q_{L1}}{Q_1}$$

where

$Q_1 = \dot{m}_\ell h_{fg}$

$\dot{m}_\ell$ = total mass flow rate

h_{fg} = heat of vaporization

Q_{L1} = heat loss from boiler to test section measured for (1)

However, this is the quality at the entrance to the test section. An amount of heat is lost by the vapor in traversing the test section. This can be estimated on the basis of free convection from the calorimeter case to the surrounding air. With this correction, the average quality for the pressure drop run is given by:

$$\bar{x}_v = \frac{Q_1 - Q_{L1} - Q_{L2}/2}{Q_1}$$

where

Q_{L2} = heat loss from test section to calorimeter case

For the test results presented in Sec. 2.5, the flowmeter of Fig. 2-1 was replaced by weighing the outlet flow.

In order to estimate the accuracies involved, two additional tests were run:

1. Superheated vapor was run through the test section with the cooling air shut off. Pressure drop, temperature, and flow rate (out of a downstream condenser) were recorded. The

results were then compared to the pressure drop predicted by single phase theory. The test results had a maximum deviation of 6 percent from the calculated pressure drop.

2. Superheated vapor was condensed in the test section (cooling air on). The flow rates and temperatures of mercury and air were recorded. The calculated heat content of the vapor was then compared to the heat absorbed by the cooling air. The maximum deviation of measured vapor heat content from that calculated was 3 percent.

In view of the above tests it is estimated that the pressure drop and flow rate data have a maximum uncertainty of approximately $\pm$ 10 percent.

2.5 <u>Test Results</u>

Test results for the geometry investigated are shown in Fig. 2-2. The ordinate of the curve is Φ_v^2, the ratio of two-phase pressure drop (measured pressure drop) to that which would occur if the vapor phase were flowing alone (calculated). This parameter is plotted vs. X_{vt}^2 which is defined as the ratio of the pressure drop which would occur if the liquid phase were flowing alone to that which would occur if the vapor phase flowed alone. This quantity involves the ratio of liquid to vapor flow rate (measured) multiplied by empirical factors from the Fanning equation.

The subscript, vt, refers to the flow mechanism which Martinelli defines (Ref. 5). For this case the flow mechanism is turbulent vapor phase (Re_v = 6000-9000) and laminar liquid phase (Re_L < 2000). X_{vt}^2 was increased by decreasing the inlet quality of the vapor. Average quality was varied from 1.0 to 0.515. The points at X_{vt}^2 = 0 are for single phase vapor flow. Other test conditions are summarized on the curve and tabulated in Table 2-1.

Two very significant results are apparent in Fig. 2-2:

1. Introduction of a small amount of the liquid phase in flowing mercury vapor causes a rapid increase in pressure drop.

TABLE 2-1

Date 4/18-5/3 Time

TEST DATA SHEET

Test Number

Subject Two Phase Mercury Pressure Drop W.A. 1588 Observed by L. Hays

ELECTRO-OPTICAL SYSTEMS, INC.

Purpose of Test

Obtain isothermal pressure drop data for two phase mercury flow.

Description of Setup

A straight tube test section was tested

Pressure taps located at 16-1/4" distance

Tube I.D. = 0.137"

Tube Material / 304 SS

Outer air jacket instrumented for air temp and flow rate and insulated.

Changes since previous test

Elimination of [illegible] test section.

Note: $\bar{R}_{Re_v}$ = average vapor Reynolds No.

f_{v_c} = friction factor if vapor were flowing alone

Δp_{v_c} = calculated Δp if vapor were [illegible]

Data Run No.	Total flowrate [illegible]	Quality at [illegible]	Average Quality	$\bar{R}_{e_v}$	f_{v_c}	Vapor Velocity [illegible]	Δp_{vc} [illegible]	Δp_{meas} (psf)	Δp_{mom} (psf)
M1	15.5	1.0	1.0	7870	.0326	147 fps	247psf	232	0
M2	15.6	1.0	1.0	8030	.0324	146	246	244	0
M3	14.6	1.0	0.960	9170	.0312	104	151	183	7.8
M4	18.4	--	0.710	8550	.0316	96.4	132	209	7.9
C4	19.1	0.759	--	--	--	--	--	--	--
M5	17.9	--	0.762	8910	.0314	101	143	198	8.0
C5	17.4	0.790	--	--	--	--	--	--	--
M6	17.3	--	0.748	8450	.0316	95.4	130	192	7.8
C6	17.0	0.786	--	--	--	--	--	--	--
M7	19.6	--	0.507	6500	.0346	73.2	83.4	183	6.0
C7	20.5	0.564	--	--	--	--	--	--	--

1588-20-1

EOS Form [illegible]

Date 4/18-5/3 Time

Test Number

TEST DATA SHEET

Subject: Two Phase Mercury Pressure Drop W.A. 1588 Observed by L. Hays

ELECTRO-OPTICAL SYSTEMS, INC.

Run No.	Vapor Inlet Temperature	Vapor Inlet Pressure	Outlet Temperature	Cooling air flow Rate	Cooling air ΔT	ϕ_v^2	X_{vt}^2		
M1	1245°F	~16 psia	705°F	0	0	0.983	0		
M2	1209	"	708	0	0	0.940	0		
M3	780	"	670	0	0	1.27	52×10^{-4}		
M4	688	"	672	0	0	1.64	5.43×10^{-4}		
C4	680	"	660	25 cfm	68°F	--	--		
M5	685	"	672	0	0	1.44	3.97×10^{-4}		
C5	680	"	510	25	68	--	--		
M6	685	"	[illegible]	0	0	1.3[illegible]	[illegible]$.62\times10^{-4}$		
C6	680	"	450	25	68	--	--		
M7	630	"	674	0	0	1.65	6.3×10^{-4}		
C7	683	"	[illegible]	24	68	--	--		

1588-2Q-1

EOS Form No. 247

For example, the test point at X_{vt}^2 = .9[illegible] corresponds to an average quality through the test section of 0.96, but the pressure drop is about 1.3 times that which would result for single-phase vapor.

2. A fair agreement exists between the test data and Martinelli's curve which was established for isothermal flow for fluids other than mercury. The maximum deviation of the test data from Martinelli's curve is 1[illegible] percent if the deviation is referenced to X_{tt}^2 = 0. This is within the deviation of the data Martinelli correlated ($\pm$ 50 percent).

It should be emphasized again that very little condensation (and pressure recovery) occurred during the pressure drop runs. This condition constitutes the principal change between the present tests and those run previously with transparent test sections and with condensing flow. In the present tests, the pressure recovery correction is less than 4 percent.

The present test results indicate the correlation of Martinelli to be valid for two-phase isothermal mercury flow for the variables investigated. Possibly, if the correlation is examined for a wider range of variables, the means for accurate prediction of pressure drop in a direct condenser using mercury can be established and verified.

[illegible].5 Future Effort

In order to completely establish the pressure drop criterion to be used in mercury condensers, the test procedure described above should be used to investigate an extended range of flow conditions and geometries. With proper selection of test conditions and geometries, the major uncertainties associated with other measurements can be eliminated and a firm correlation established. Any further investigation should probably include larger tube sizes (at least 1/2") and possibly that ejection rate (isothermal to extremely rapid rates) in order to bracket existing designs. Moreover, the investigation should be instrumented to measure pressure differences [illegible] wall locations.

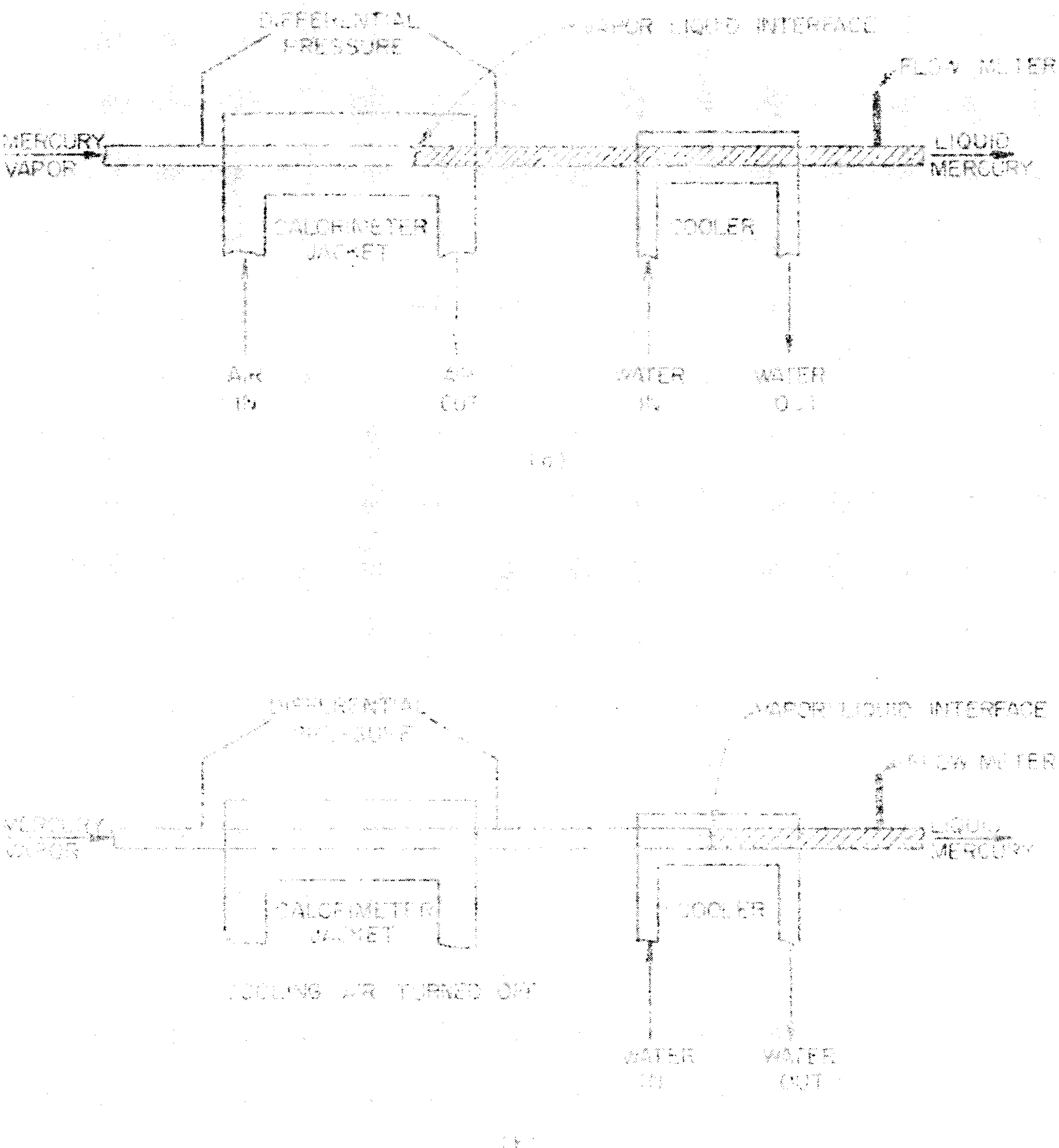

FIGURE 2-1 SCHEMATIC REPRESENTATION OF [illegible]

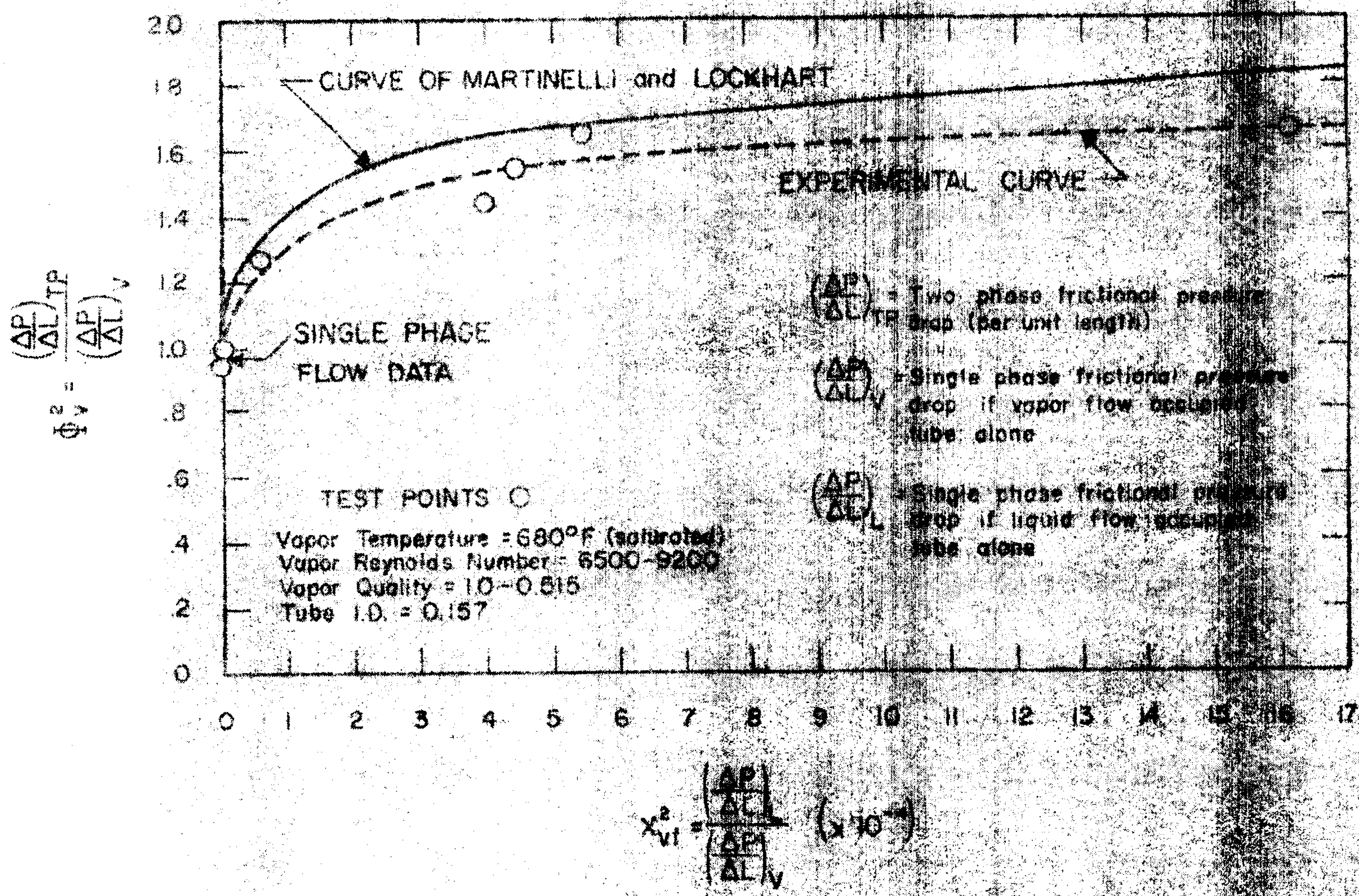

FIG. 2-2 RATIO OF TWO PHASE PRESSURE DROP TO VAPOR PRESSURE DROP VS. RATIO OF LIQUID TO VAPOR PRESSURE DROP FOR NEARLY ISOTHERMAL TWO PHASE SINGLE COMPONENT FLOW OF MERCURY

Section 3
NOMENCLATURE

A	Area, ft^2
D	[illegible]
E	[illegible] energy,
g	gravitational constant, 32.2 ft/sec^2
h	enthalpy (includes heat of vaporization when it refers to vapor)
J	Mechanical equivalent of heat, 778 ft-lb/btu
$\dot{m}$	Flow rate, lb/sec
p	pressure, lb/ft^2
R	Specific gas constant, $ft/^{\circ}R$
s	entropy, $Btu/lb\,^{\circ}R$
T	Temperature, $^{\circ}R$
V	Velocity, ft/sec
v	specific volume, ft^3/lb
x	quality, weight - fraction of vapor in a saturated vapor-liquid mixture, mass flow ratio
ρ	density, lbs/ft^3

Subscripts

f	Saturated liquid
L	Liquid
v	Saturated vapor
1,2,3,4	stations in condensers, defined in each section.

3. SPRAY CONDENSER ANALYSIS

One of the advantageous characteristics of a spray condenser for use in a Rankine cycle power system is its pressure augmentation capability. With proper design a significant pressure rise may be added to the condensing vapor. This pressure augmentation is desirable in order to suppress pump cavitation and to minimize the pumping power required to inject the subcooled liquid into the spray condenser.

As discussed previously, constant area spray condensers were investigated at Electro-Optical Systems on Contract DA-04-495-506-ORD-2007 and during the first period of the present contract. For this type of test section, operating with mercury, pressure increments up to 188 psf were obtained (Ref. 1). Use of a properly designed convergent-divergent geometry will provide even higher pressure increments. This effect can be explained qualitatively with the aid of the photographs (Ref. 1) of condensation in a constant area tube. The vapor liquid interface associated with condensation on a central jet or spray is accompanied by a sudden expansion. The flow process is somewhat analogous to a sudden expansion in a pipe in single phase flow and is accompanied by a relatively inefficient recovery of kinetic energy. However, if the mixing chamber is contoured to effect condensation with little reduction in jet or spray kinetic energy, and if a diverging section is added for efficient diffusion, the pressure increment added to the vapor pressure is increased.

In order to compare the performance of constant and variable area spray condensers, simplified analyses were made. These analyses provide the basis for selection of test section geometry and extension of test results to other geometries.

3.1 Constant Area Calculations

The model used for constant area calculations is shown below.

Vapor and liquid are injected at station 1. Condensation of the vapor takes place as the flow proceeds downstream. The injected liquid serves as a heat and mass sink for the condensing vapor. At some point within the control volume (bounded by the dashed boundary), a vapor-liquid interface occurs. The exit point, designated by the subscript 2, is defined as the downstream station where the flow is homogeneous (but not necessarily all liquid) and in thermal equilibrium. The radial pressure profile at the end points is taken to be constant and wall friction is neglected. Furthermore, the assumption is made that the saturated liquid (quality less than 1) associated with the entering vapor is traveling at the same velocity as the vapor (no "slip"). Using these assumptions the equation of conservation of momentum for the control volume becomes:

$$\frac{\dot{m}_{L_1} V_{L_1}}{g} + \frac{\dot{m}_{\ell_1} V_{V_1}}{g} + \frac{\dot{m}_{V_1} V_{V_1}}{g} + p_1 A = \frac{\dot{m}_{L_2} V_2}{g} + \frac{\dot{m}_{V_2} V_2}{g} + p_2 A \qquad 3\text{-}1$$

Using the above terms, the quality at station 1 is defined as

$$x_1 = \frac{\dot{m}_{V_1}}{\dot{m}_{V_1} + \dot{m}_{\ell_1}} \qquad 3\text{-}2$$

In terms of quality, equation 3-1 becomes

$$\frac{\dot{m}_{L_1} V_{L_1}}{g} + \frac{\dot{m}_{V_1} V_{V_1}}{g}\left(\frac{1}{x_1}\right) + p_1 A = \frac{\dot{m}_{L_2} V_{L_2}}{g}\left(\frac{1}{1-x_2}\right) + p_2 A \qquad 3\text{-}3$$

For complete condensation it follows that $x_2 = 0$ and equation 3-3 becomes

$$\frac{\dot{m}_{L_1} V_{L_1}}{g} + \frac{\dot{m}_{V_1} V_{V_1}}{g}\left(\frac{1}{x_1}\right) + p_1 A = \frac{\dot{m}_{L_2} V_{L_2}}{g} + p_2 A \qquad 3\text{-}4$$

But

$$\dot{m}_{L_2} = \dot{m}_{L_1} + \frac{\dot{m}_{V_1}}{x_1} \qquad 3\text{-}5$$

$$\dot{m}_{L_1} = \rho_{L_1} A_{L_1} V_{L_1} \qquad 3\text{-}6$$

and

$$\dot{m}_{V_1} = \rho_{V_1} A_{V_1} V_{V_1} \qquad 3\text{-}7$$

Substituting equations 3-5, 3-6, and 3-7 into equation 3-4 gives

$$\frac{\Delta p}{\frac{\rho_{V_1} V_{V_1}^2}{g}} = \frac{p_2 - p_1}{\frac{\rho_{V_1} V_{V_1}^2}{g}} = \frac{\left[\left(\frac{\rho_L}{\rho_{V_1}}\right)\left(\frac{V_{L_1}}{V_{V_1}}\right)^2\right]\left[1 + \left(\frac{1}{x_1}\,\frac{\dot{m}_{V_1}}{\dot{m}_{L_1}}\right)\left(\frac{V_{V_1}}{V_{L_1}}\right) - \frac{\left(\frac{1}{x_1}\,\frac{\dot{m}_{V_1}}{\dot{m}_{L_1}} + 1\right)^2}{1 + \left(\frac{\dot{m}_{V_1}}{\dot{m}_{L_1}}\,\frac{V_{L_1}}{V_{V_1}}\right)\left(\frac{\rho_L}{\rho_{V_1}} + \frac{1-x_1}{x_1}\right)}\right]}{1 + \frac{\dot{m}_{V_1}}{\dot{m}_{L_1}}\,\frac{V_{L_1}}{V_{V_1}}\left(\frac{\rho_L}{\rho_{V_1}} + \frac{1-x_1}{x_1}\right)} \qquad 3\text{-}8$$

The last term of Equation 3-8 is the non-dimensional pressure rise [illegible]

[illegible] to be [illegible], which corresponds to [illegible] mercury [illegible]. Equation [illegible] fluid, [illegible] is fixed by the fluid in the density ratio.

[illegible]

kinetic energy of the vapor were converted to pressure.

However, this magnitude of pressure rise would occur for low values of velocity ratio (~1); for representative values (~20), lower pressure rises result. As an example, for a vapor velocity of 300 fps, liquid velocity of 15 fps, and area ratio of 0.20 from Fig. 3-1:

$$\frac{\Delta p}{\rho_v V_{v_1}^2/g} = 1.8$$

The absolute magnitude of Δp would be

$$\Delta p = \frac{(.25)(300)^2(1.8)}{(32.2)(144)} = 10.1 \text{ psi}$$

Thus it would be possible for this case to add about 10 psi to the condenser inlet pressure of 20 psi (if no wall friction losses are considered). Results of testing constant area spray tubes with mercury have resulted in

values of pressure rise of this order of magnitude. In general, test results have approached the results of the analysis within 20 percent.

In order to determine the effect of noncondensed vapor on [illegible]

[illegible]

3-3 yields

$$\frac{\Delta P}{\rho_{V_2} V_{V_1}^{2}} = \frac{1 + \left(x_1 \frac{A_{L_1}}{A_{V_1}}\right) \frac{V_{L_1}}{V_{V_1}} - \frac{m_{L_2}}{m_{V_1}} \frac{V_{L_2}}{V_{V_1}} \left(\frac{1}{1-x_2}\right)}{\frac{m_{L_1}}{} \; \frac{V_{V_1}}{} \; \frac{\rho_{V_1}}{} \;[illegible]\; 1 + \frac{}{1 + \frac{\rho_{V_1}}{\rho_L}\left(\frac{1-x_1}{x_1}\right)}} \qquad 3\text{-}9$$

[illegible] results in the following expression for the velocity ratio

$$\frac{V_{L_2}}{V_{V_1}} = \frac{(1-x_2)\left(\frac{\frac{\rho_{V_1}}{\rho_L}}{1 + \frac{\rho_{V_1}}{\rho_L}\left(\frac{1-x_1}{x_1}\right)} + \left(\frac{A_{L_1}}{A_{V_1}}\right)\left(\frac{V_{L_1}}{V_{V_1}}\right)\right) + x_2\left(\frac{\rho_{V_1}}{\rho_{V_2}} + \frac{\rho_L}{\rho_{V_2}}\left(\frac{A_{L_1}}{A_{V_1}}\right)\left(\frac{V_{L_1}}{V_{V_1}}\right)\right)}{1 + \left(x_1 \frac{m_{L_1}}{m_{V_1}}\right)\left(\frac{V_{V_1}}{V_{L_1}}\right) \frac{\rho_{V_1}/\rho_L}{1 + \frac{\rho_{V_1}}{\rho_L}\left(\frac{1-x_1}{x_1}\right)}} \qquad 3\text{-}10$$

where

$$\frac{A_{L_1}}{A_{V_1}} = \left(\frac{m_{L_1}}{m_{V_1}}\right)\left(\frac{\rho_{V_1}}{\rho_L}\right)\left(\frac{V_{V_1}}{V_{L_1}}\right) \qquad 3\text{-}11$$

and

$$\rho_{v_2} = f(P_2) \qquad \text{3-12}$$

Solution of equation 3-9 using the subsidiary equations 3-10 and 3-11 yields the nondimensional pressure rise for arbitrary values of x_2. An iterative method of solution [illegible] results for a representative case. Figure 3-2 presents the effects of noncondensed vapor on nondimensional pressure rise for the following initial conditions.

$$\frac{\dot{m}_{L_1}}{\dot{m}_{v_1}} = 10 \qquad \frac{V_{v_1}}{V_{L_1}} = 10$$

$$\frac{\rho_L}{\rho_{v_1}} = 2620 \qquad x_1 = 1$$

The pressure rise is strongly affected by noncondensed vapor. For example, for the above conditions 2 percent vapor at station 2 results in a reduction in the nondimensional pressure rise from 1.9, (for the case of complete condensation) to a value of -0.70. For this particular case, the volume flow ratio (vapor-to-liquid) is approximately 60 so that the occurrence of an interface with homogenous flow conditions at station 2 is probably not a realistic assumption. However, curves of this type can be used to estimate deviations from theoretical pressure rise for a small amount of noncondensed vapor.

3.2 <u>Variable Area Spray Condensers</u>

The conservation equations were applied to the processes occurring in condensation in a converging spray tube section. However, without assumptions of the rates and mechanisms of the mass, energy and momentum exchange occurring, the equations are not solvable. Moreover, depending on the assumptions made, significantly different results can occur from the analysis. Therefore, three alternative models were examined. Test results will be used in an effort to select the most applicable.

1. For the first model, constant pressure is assumed to exist throughout the length of the converging section in both the liquid and vapor. Moreover, the same pressure was assumed to exist at the throat of the condenser or the [illegible] actual constant pressure along the integral of pressure around the control contour is zero.
2. The second model incorporates an isentropic expansion of the liquid-vapor mixture with equilibrium condensation occurring in the converging section. For this case, the properties of the injected liquid are assumed to remain constant. A condensation shock is then assumed to occur at the throat region of the condenser.
3. The constant pressure jump model incorporated constant pressure condensation in the converging section as did the first. However, for this case, a pressure rise is taken to occur across the vapor-liquid interface.

In order to maintain constant pressure in the liquid after complete condensation of the vapor, the throat area may be smaller than the area of the injected liquid for some initial conditions. Use of such a geometry would result in "choked flow" occurring at the throat or immediately before it. This consideration has the effect of limiting the applicability of the results obtained from the constant pressure model. The second model takes sonic flow conditions into consideration and terminates the converging section at the place at which sonic flow occurs. However, the assumption of equilibrium condensation occurring does not appear to agree with temperature probes which have been made in the liquid jet of spray tubes. The third model may be closer to physical reality and offers information on the effect of varying the ratio of throat area to the area of the injected liquid.

In all three models, a diffuser is used to efficiently recover pressure. The exit area in every case is specified equal

to the entrance area of the spray condenser. This assumption allows a comparison between the pressure rises obtainable in these three cases with the constant area case.

[illegible]

below are analyzed.

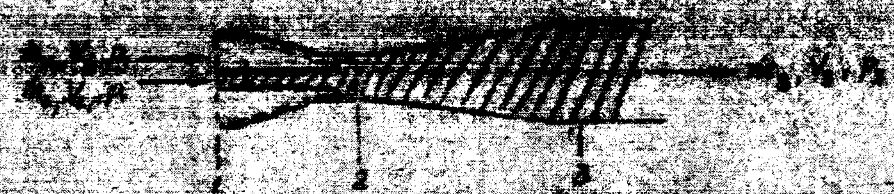

Vapor and liquid are injected simultaneously at station 1. The vapor and liquid flow concurrently [illegible] interface occurs some-where between stations 1 and 2 [illegible] is assumed to be completely condensed. The resultant liquid is then diffused from the velocity at station 2 to that corresponding to the area at station 3 (which is equal to the inlet area).

For the constant pressure model, the pressure area terms in equation 3-1 cancel with the pressure integral along the wall. The equation then becomes

$$\frac{\dot{m}_{L_1} V_{L_1}}{g} + \frac{\dot{m}_{V_1} V_{V_1}}{g} + \frac{\dot{m}_{V_1} V_{V_1}}{g} = \frac{\dot{m}_{L_2} V_2}{g} + \frac{\dot{m}_{V_2} V_2}{g} \qquad 3\text{-}12$$

With the inlet flow expressed in terms of quality, equation 3-12 may be rearranged to give

$$\frac{V_2}{V_{L_1}} = \frac{\left(1-x_2\right) \left[\frac{\dot{m}_{L_1}}{\dot{m}_{V_1}} + \frac{1}{x_1} \quad \frac{V_{V_1}}{V_{L_1}}\right]}{\frac{\dot{m}_{L_1}}{\dot{m}_{V_1}} + \frac{1}{x_1}} \qquad 3\text{-}13$$

Incorporation of the conservation of mass leads to the following expression for the ratio of throat area to inlet area.

1588-20-1

$$A_2\left(\frac{1}{x_1} + \frac{\dot m_{L_1}}{\dot m_{V_1}}\right)\left(\frac{V_{V_1}}{\ldots}\right) \ldots + x_2\left(\frac{\rho_L}{\rho_{V_1}} - 1\right) \ldots$$

[illegible]

[illegible] low values [illegible] vapor to liquid velocity and low values of the [illegible] very low [illegible]

[illegible] Applying

$\dfrac{\rho_{V_1} V_{V_1}^2}{g}$ [illegible] $\dfrac{\rho_{V_1} V_{V_1}^2}{g}$

Bernoulli's equation(since single phase flow is occurring and the streamlines are continuous) between stations 2 and 3 results in the following equation.

$$\frac{P_3 - P_1}{\dfrac{\rho_{V_1} V_{V_1}^2}{g}} = \left(\frac{\rho_L}{\rho_{V_1}}\right)\left(\frac{V_L}{V_{V_1}}\right)^2 \left[\left(\frac{V_2}{V_{L_1}}\right)^2 - \left(\frac{V_3}{V_{L_1}}\right)^2\right] \qquad 3\text{-}15$$

where

$\dfrac{V_2}{V_{L_1}}$ is given by equation 3-13 and

$$\frac{V_3}{V_{L_1}} = \frac{\dfrac{\dot m_{L_1}}{\dot m_{V_1}} + \dfrac{1}{x_1}}{\left(\dfrac{\dot m_{L_1}}{\dot m_{V_1}} + \dfrac{V_{L_1}}{V_{V_1}}\right)\left(\dfrac{\rho_L}{\rho_{V_1}} + \dfrac{1-x_1}{x_1}\right)} \qquad 3\text{-}16$$

Equation 3-15 is plotted vs. mass flow ratio in Fig. 3-4 for inlet conditions which are identical to the previously

$$\frac{\rho_{L_1}}{\rho_{V_1}} = 2620$$

Figure 3-1 for the constant area geometry gives a predicted non-dimensional pressure rise of about 1.8. The constant pressure calculations (Fig. 3-4) predict a nondimensional pressure rise of about 31 for the same inlet conditions.

3.2.2 Isentropic Expansion Model

[illegible]

[illegible]

Figure [illegible] component section [illegible] of isentropic [illegible] occurring while the condition [illegible] Between stations 2 and 3 [illegible] is then diffused to station 4 where area is equal to the inlet area. Consider only isentropic expansion of the liquid vapor mixture.

$$\dot{m}_{V_1}\left(S_{V_1} + \frac{1-x_1}{x_1} S_{F_1}\right) = \left(S_{V_2} + \frac{1-x_2}{x_2} S_{F_2}\right)\dot{m}_{V_2} \qquad 3\text{-}16a$$

Solving for x_2:

$$x_2 = \frac{x_1 S_{V_1} + \left(1-x_1\right) S_{F_1} - S_{F_2}}{S_{V_2} - S_{F_2}} \qquad 3\text{-}17$$

For a given set of initial conditions, x_2 is a function of T_2 only, and

$$\dot{m}_{V_1} h_{V_1} + \dot{m}_{F_1} h_{F_1} + \left(\dot{m}_{V_1} + \dot{m}_{F_1}\right)\frac{V_{V_1}^2}{2gJ} = \dot{m}_{V_2} h_{V_2} + \dot{m}_{F_2} h_{F_2} + \left(\dot{m}_{V_2} + \dot{m}_{F_2}\right)\frac{V_{V_2}^2}{2gJ} \qquad 3\text{-}18$$

Solving equation 3-18 for V_{V_2}:

$$[illegible] \qquad 3\text{-}19$$

From the equation of continuity,

$$\frac{A_2 - A_{L_2}}{A_1 - A_{L_1}} = \frac{V_{V_1}}{V_{V_2}}\left(\frac{x_2 v_{v_2} + (1-x_2) v_{F_2}}{x_1 v_{v_1} + (1-x_1) v_{F_1}}\right) \qquad 3\text{-}20$$

where specific volume v is a function only of temperature and $A_{L_1} = A_{L_2}$ [illegible] is also as a function of [illegible]. Thus, the thermodynamic properties at station 2 may be found as functions of one variable such as $\frac{A_2}{A_1}$.

2. For the case of complete condensation, ($x_3 = 0$), the constant area analysis in section 3.1 can be used to calculate properties at station 3. Since p_{L_2} is not equal to p_{V_2}, the average pressure at station 2 was used in calculating the pressure rise. The average pressure at station 2 is given by

$$p_2 = \frac{A_{L_2} p_{L_2} + A_{V_2} p_{V_2} + A_{F_2} p_{F_2}}{A_2} \qquad 3\text{-}21$$

where

$$p_{V_2} = p_{F_2} \qquad 3\text{-}22$$

In the application of the results of the constant area analysis, subscripts 1 and 2 should be changed to 2 and 3 respectively. The velocity at station 3 is found from the conservation of mass to be

$$V_3 = V_{L_1}\left[\frac{\frac{1}{x_1} + \frac{\dot{m}_{L_1}}{\dot{m}_{V_1}}}{\left(\frac{\dot{m}_{L_1}}{\dot{m}_{V_1}}\right)\left(\frac{A_2}{A_{L_1}}\right)}\right] \qquad 3\text{-}23$$

and similarly

[illegible]

The curve is terminated at the value of area ratio which would result in a Mach number of 1 for the expanding vapor. Nondimensional pressure rise increases as lower values of throat to inlet area ratio are approached. This is due to the type of effect discussed in the first part of this section. The inlet conditions were chosen to be among those presented in the previous plots. Comparison of this figure with the curves obtained for the constant pressure model indicates a much lower nondimensional pressure rise and a higher value of the ratio of throat to inlet area ratio for the isentropic model than for the constant pressure model. If the throat-to-inlet area ratio resulting in the constant pressure model were used in the isentropic model, choke flow conditions would result. As an example, for the flow conditions used in the isentropic calculation, the constant pressure model predicts a pressure rise of

[redacted] calculations are currently being carried out on the third model which assumes constant pressure in the converging portion of the spray cone and a pressure discontinuity across the interface at the throat. Preliminary results indicate the calculated pressure rise to be slightly greater for this model than that obtained using the isentropic expansion model. Results are being calculated as a function of inlet conditions and as a function of throat-to-liquid area ratio.

Results of either the second or third model will be used to select converging-diverging test sections. Results of testing these sections will then be related to the pressure rise and area ratios predicted by both of these models in order to determine which is more applicable to the processes occurring in convergent-divergent spray tubes.

1588-2Q-1

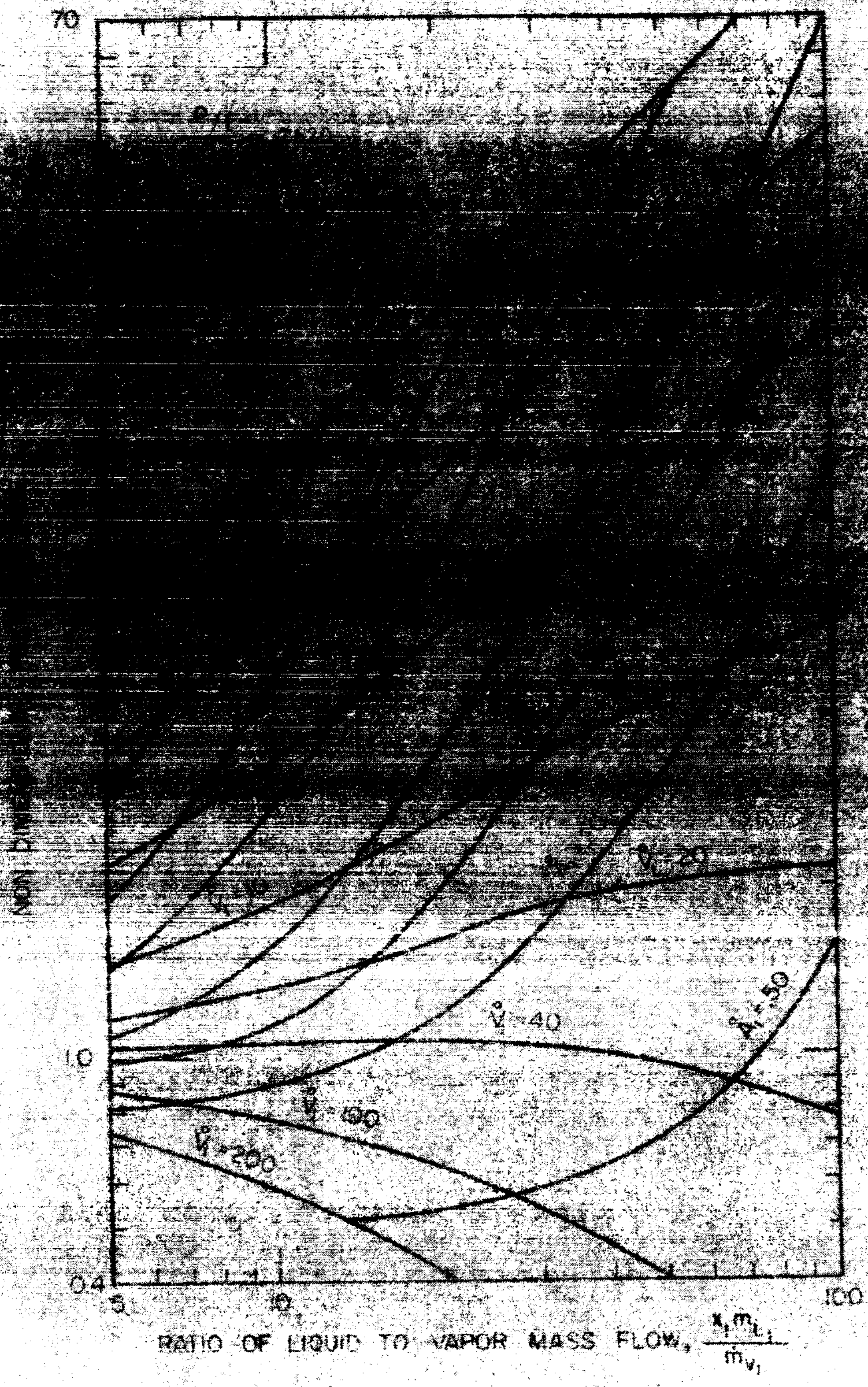

FIG. 3-1 CALCULATED PRESSURE RISE EFFICIENCY VS. MASS FLOW RATIO FOR CONSTANT AREA CONDENSATION OF MERCURY VAPOR

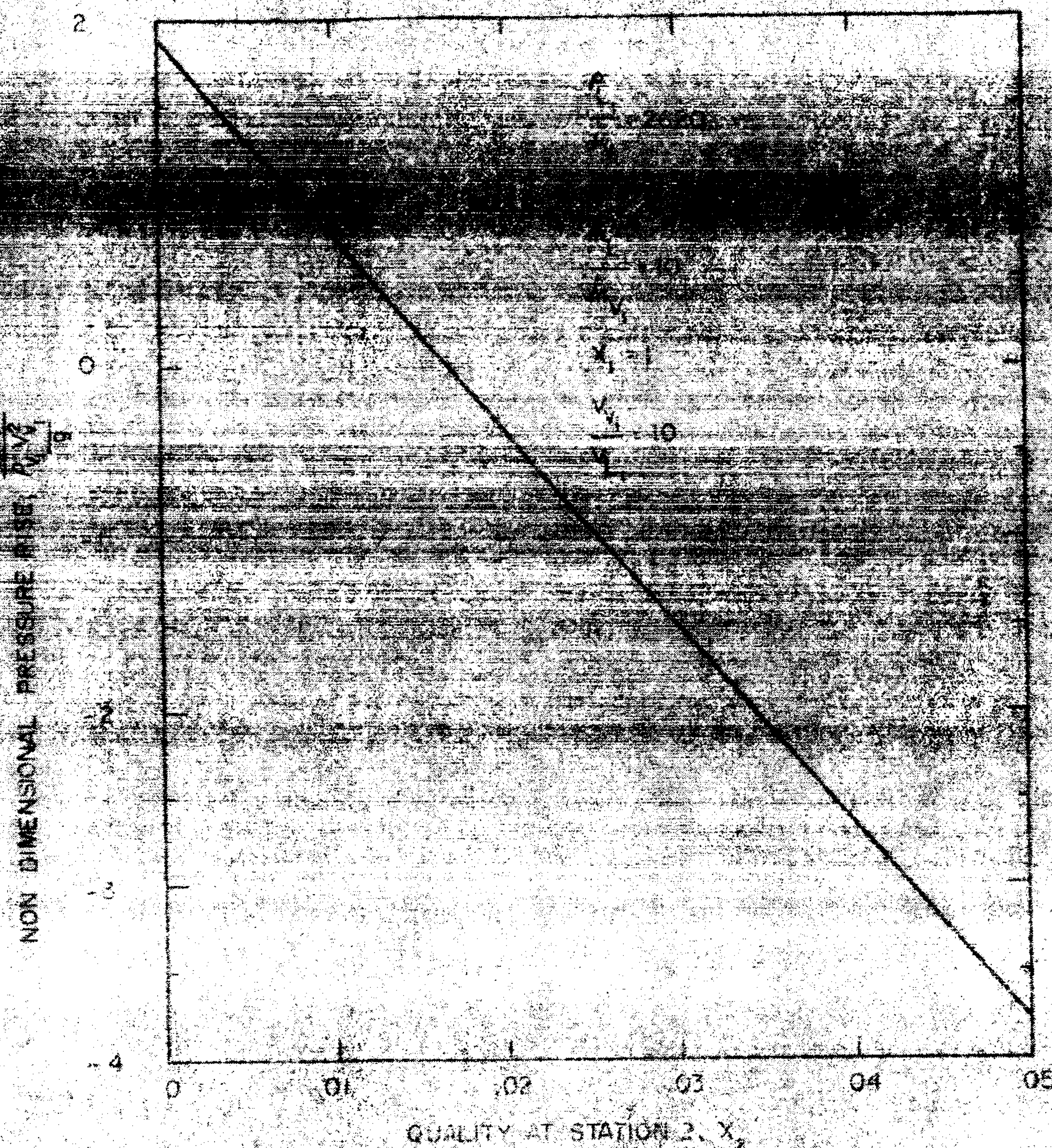

FIG. 3-2 EFFECT OF UNCONDENSED VAPOR ON PRESSURE RISE IN CONSTANT AREA CONDENSER

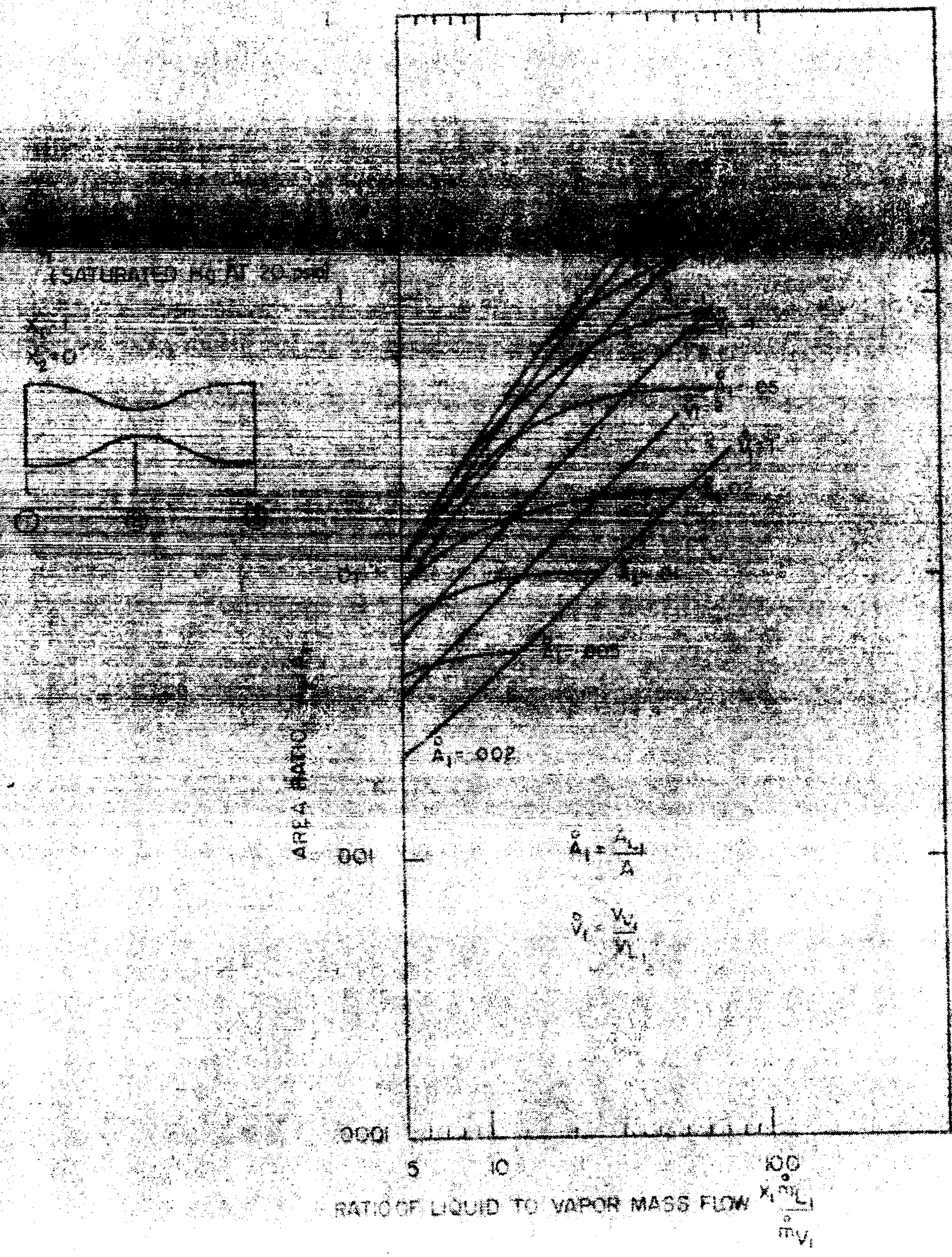

FIG. 3-3 VARIATION OF THROAT AREA RATIO FOR A CONSTANT PRESSURE CONDENSER WITH A DIVERGING SECTION

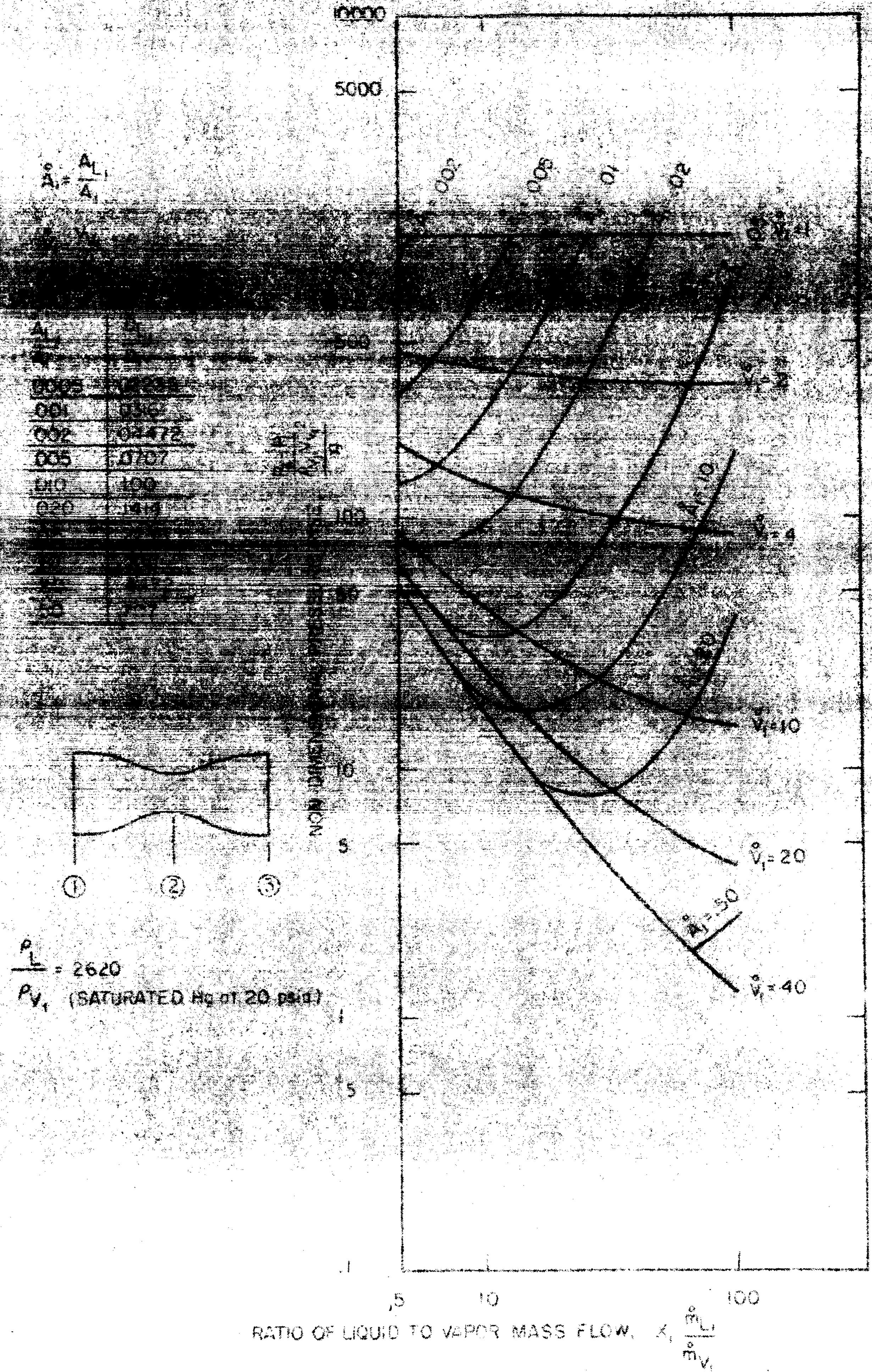

FIG. 3-4 PRESSURE RISE IN CONSTANT PRESSURE CONDENSER WITH DIVERGING SECTION

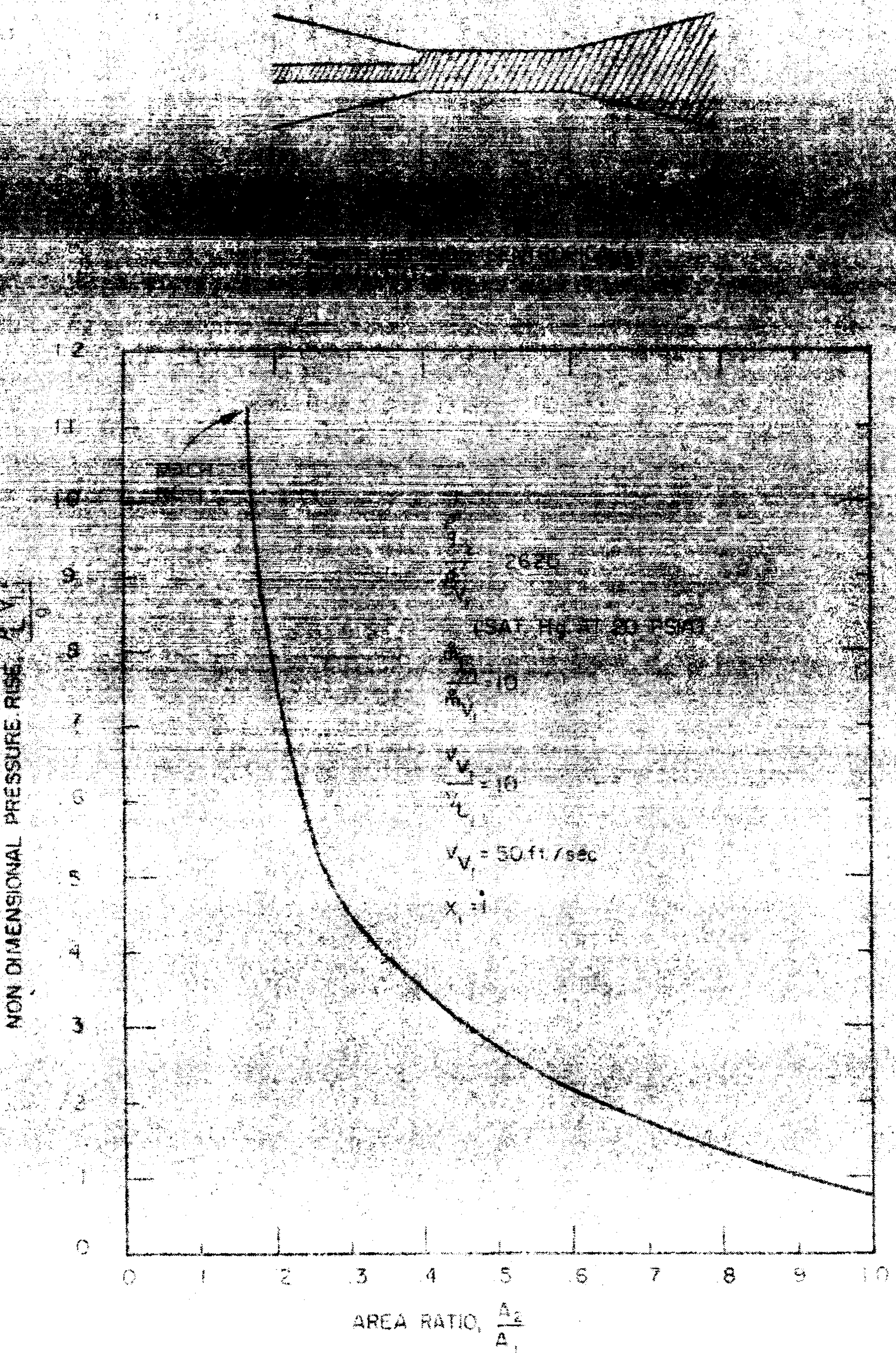

FIG. 3-5 EFFECT OF THROAT AREA RATIO ON PRESSURE RISE IN CONVERGING-DIVERGING SPRAY CONDENSER

[illegible] (Ref. 1) has [illegible] demonstrated with these test units. However, the use of small orifices to inject the subcooled liquid has [illegible] features associated with [illegible]. In order to [illegible]

Subcooled liquid is injected in the form of a central jet which flows concurrently with the vapor. Vapor condensed continuously on the jet until at some point a vapor-liquid interface forms.

Two test sections were chosen from the analysis in Sec. 3 for investigation. Their dimensions are given in Table 4-1. No difficulty was encountered in testing the unit with an area ratio of .072. However, the geometry with an area ratio of 0.20 exhibited non-uniform liquid flow due to obstruction of vapor flow caused by the injector. Both sections were tested with the existing test loop and with vapor thermodynamic and flow conditions similar to those used previously for multiple jets. The test data will be tabulated in the final report.

4.2 Experimental techniques.

The same general procedure used in previous tests (Ref. 1) was used for central injector geometries. The most important exception, however, was that a vapor quality equal to 1 at the inlet to the test

TABLE [illegible]

Test Section [illegible]

Test Section No.	Type	Spray Inside Tube Diameter	[illegible]	[illegible]	[illegible]	[illegible] Transparent Mixing Chamber Length
3	Central Injector	0.190"	[illegible]	[illegible]	[illegible]	[illegible]
4	Central Injector	0.190"	[illegible]	[illegible]	[illegible]	[illegible]

section was established for every test run. In order to insure a quality [illegible]

[illegible]	[illegible]
Pressure (differential)	± .1 psid
Orifice Liquid Flowmeters	± 2 °/o full scale
Temperatures	± 2°F
Recorder	± 8°F (calibrated)
Air Flowmeter	± 1 cfm
Interface Distance	± 1/16"

A schematic of the test loop, together with the locations of the important measurements, is shown in Ref. 1.

4.3 Range of Variables

A summary of the range of variables tested is shown in Table 4.3. The most important of these variations were vapor flow rate (by a factor of about 2) and mass flow ratio of liquid to vapor (by a factor of about 5.) These variations enabled an empirical correlation of data to be made, (see Sec. 4.4), which can be used as a preliminary basis for extending the test results to other geometries and flow conditions. The maximum vapor velocity ($\sim$150 fps) and mass flow ratio (30-60 depending on vapor flow) possible with the existing test facility were

TABLE 4-3

RANGE OF VARIABLES FOR MERCURY SPRAY CONDENSER TESTS

[illegible]	[illegible]
Liquid flow rate	370-[illegible] lb/hr
[illegible]	[illegible]
[illegible]	[illegible]

provide data which can be applied to current system designs.

[redacted]

can be directly related to X'. This will be done in the future.

Curves of condensation length vs. spray utilization factor are shown in Fig. 4-1. A significant feature of each curve is the appearance of the three regions. In the first region, large changes in spray utilization factor can occur with very little effect on condensation length. The second region represents a transition zone where changes in spray utilization factor produce changes of an equal magnitude in condensation length. In the third region (which should be avoided in operation of a spray condenser in a power system), small changes in spray utilization factor can produce very large changes in condensation length. As an example, in Fig. 4-1, for the curve to the extreme right, the first region on the curve extends from a spray utilization factor of 0 to about 0.7. The second region corresponds to a range of spray utilization factor from 0.7 to 0.87. The third region

exists for a spray utilization factor greater than 0.8?. Choice of a [redacted] vapor shear.

As the liquid injected flow rate is increased with vapor flow rate held constant, longer condensation lengths occur for the same value of spray utilization factor. Curves (5) and (3) are for the same vapor velocity with mass flow ratios of 13.5 and 21 respectively. Curve (5) shows a condensation length of 3/8" at [illegible] = 0.8, while Curve (3) gives condensation length 1" for the same value of [illegible]. This variation is probably due to two effects:

1. Decreasing liquid velocity results in a larger value of the relative vapor velocity $(V_V - V_L)$ which increases vapor-liquid shear and heat transfer area.
2. Decreasing liquid velocity increases the time a given particle of liquid spends in the vicinity of the vapor. Thus, it

is able to absorb a greater amount of heat and condense more vapor in traversing a given distance.

[illegible]

[illegible] exponent. Previously work on sprays has indicated the relative velocity to [illegible]

V_v = Vapor velocity

V_L = Jet velocity

In order to examine the correlating factor as it pertains to other geometries, results obtained with a larger area ratio are also plotted on Fig. 4-2. As can be seen, there is a reasonable agreement with data obtained for the smaller area ratio. Therefore, the effects of changing area ratio (for those tested) can be interpreted as changes of relative velocities. Testing of the larger area ratio was terminated due to a mal-distribution in the vapor flow pattern due to interference of the injector. The data set shown corresponded to conditions for which this effect was not too large.

Since the curve represents all applicable data taken thus far, it is useful as a preliminary design basis for central injector spray tubes for area ratios, flow ratios, and vapor flow rates, which are similar to those tested. A possible operating point for a preliminary design would be at a value of χ' of about .75 as indicated by the dashed

line in Fig. 4-2. If this is taken as the operating point, then the

would be

for vapor quality = 1)

$$V_L = \frac{\dot m_L \; v}{\rho_L \; A_L} \qquad 4\text{-}4$$

4. Calculate condensation length from 4-1

$$L_c = .083 \; V_L$$

5. Determine $T_f - T_i$ by a heat balance

$$R_L \; \dot m_v \; C_p (T_f - T_i) = \dot m_v \; h_{fg} + C_p \; \dot m_v \left[T_v - T_f \right] \qquad 4\text{-}5$$

(for vapor quality = 1.0)

where C_p = specific heat of liquid

h_{fg} = heat of vaporization

6. Determine T_i from equation 4-2

$$T_i = T_v - \frac{(T_f - T_i)(100)^{1/4}}{(.75)(V_v - V_L)^{1/4}}$$

Thus, the operating conditions, geometry, and condensation length are determined. If the design operating point is to be chosen [illegible]

[illegible] of spray tubes for various flow conditions and geometries. The pressure rise can be [illegible] the kinetic energy of either the vapor or injected [illegible] the kinetic energy of the vapor [illegible]

[illegible] Figure [illegible] of the nondimensional pressure rise vs spray [illegible] factor for various mass flow ratios for spray tube No. 3 (cf. Table 4-1). The nondimensional pressure rise, η_r, is defined as

$$\eta_r = \frac{\Delta p}{\frac{\rho_L V_L^2}{2g}}$$

The horizontal lines in the plot represent the calculated pressure rise for no frictional losses (see Sec. 3). η_r was obtained by multiplying the value of $\frac{\Delta p}{\frac{\rho_{v_1} V_v^2}{g}}$ from Section 3 by $\frac{2\rho_{v_1}}{\rho_L}\left(\frac{V_{v_1}}{V_L}\right)^2$. As would be expected from Section 3, the value of non-dimensional pressure rise increases as the mass flow ratio of liquid-to-vapor decreases (for a constant vapor velocity). For example, for a mass ratio of 22 the highest value of η_r obtained was about 0.155. For a mass ratio of 31 the highest value obtainable was 0.127. However, the absolute magnitude of the pressure

rise can be higher for the higher mass flow ratios. For a mass ratio of [illegible]

[illegible] flow ratio [illegible] exist at a value of a spray utilization factor approximately equal to 0.7. Figure 4-1 indicates this condition corresponds to a condensation length of about 1/4 inch and an operating point which is below the transition region mentioned in Sec. 4.4. If spray utilization factor is increased, the penalty paid in pressure augmentation can be obtained from Fig. 4-3. In general, the peak values obtained for pressure rise efficiency are comparable to values obtained with single phase jet pumps (.25-.30). Moreover, the sections tested were constant area with no attempt made to optimize the downstream configuration to recover pressure. For example, the peak of the curve for flow ratio, 22, occurs at a value of η_r = .155 (which means roughly 1-1/2 psi would be recovered for 10 psi drop across the injector).

The curves shown are for a value of $\hat{A}_1$ = 0.072. Testing of the larger area ratio ($\hat{A}_1$ = 0.20) failed to furnish pressure rise information due to the large pressure drop caused by the presence of the large injector in the vapor stream.

4.6 Stability

[redacted]

Oscillations were noted to be less severe for higher values of the mass flow ratio of injected liquid to vapor. Some evaluation of the second effect on oscillations will be made during operation of the modified test loop. The magnitude of oscillations for all tests were recorded and will be presented in the tabulation of data in the final report.

Another aspect of stability which was examined was the problem of startup. A sufficient [illegible] liquid was injected into the test section initially filled with vapor. The resulting sequence of interface formation was recorded with a Fastax camera operating at 2000-4000 fps. The motion pictures are presently being studied to gain insight into the mechanisms involved in interface formation.

[illegible]			
	T (°F)	x %	V (fps) Q/A [illegible]
[illegible]	[illegible]	[illegible]	[illegible]
[illegible] $= 0.201$			
	T (°F)	x %	V (fps) Q/A [illegible]
●	730	28	127-130 3000-4100

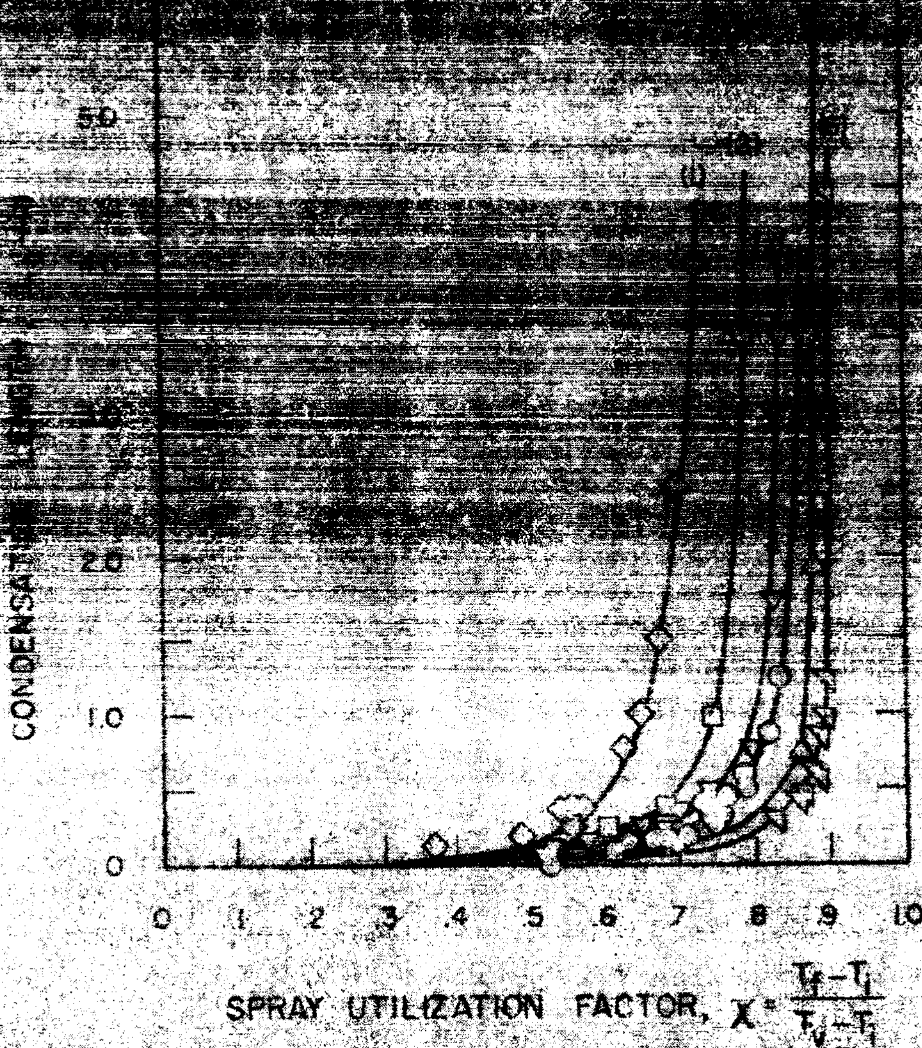

FIG. 4-1 CONDENSATION LENGTH VS. SPRAY UTILIZATION FACTOR FOR CENTRAL INJECTOR MERCURY SPRAY TUBE (δ_1 = 0.072)

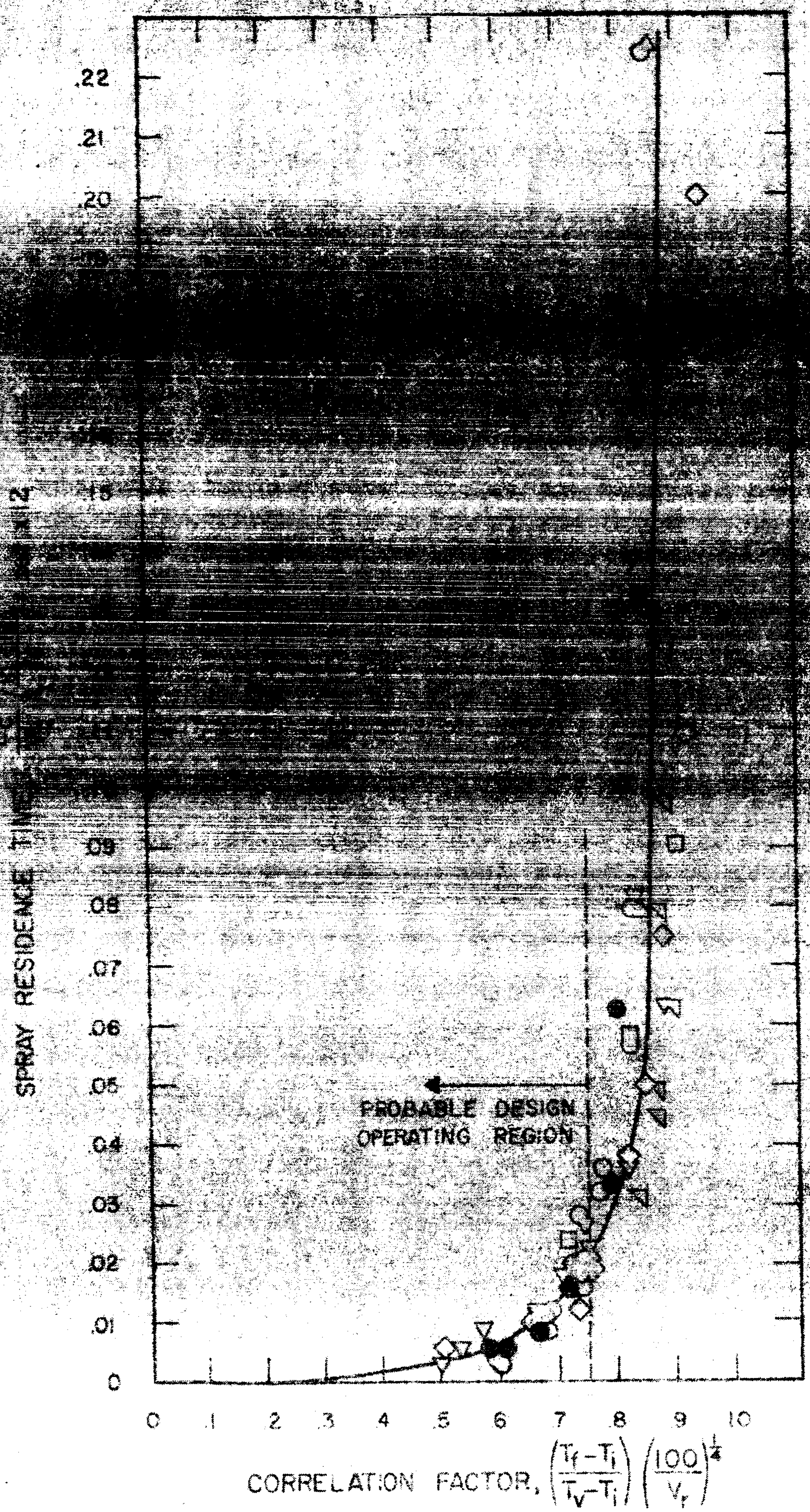

FIG. 4-2 SPRAY RESIDENCE TIME VS. CORRELATING FACTOR X' FOR CENTRAL INJECTOR SPRAY TUBES OPERATING WITH MERCURY

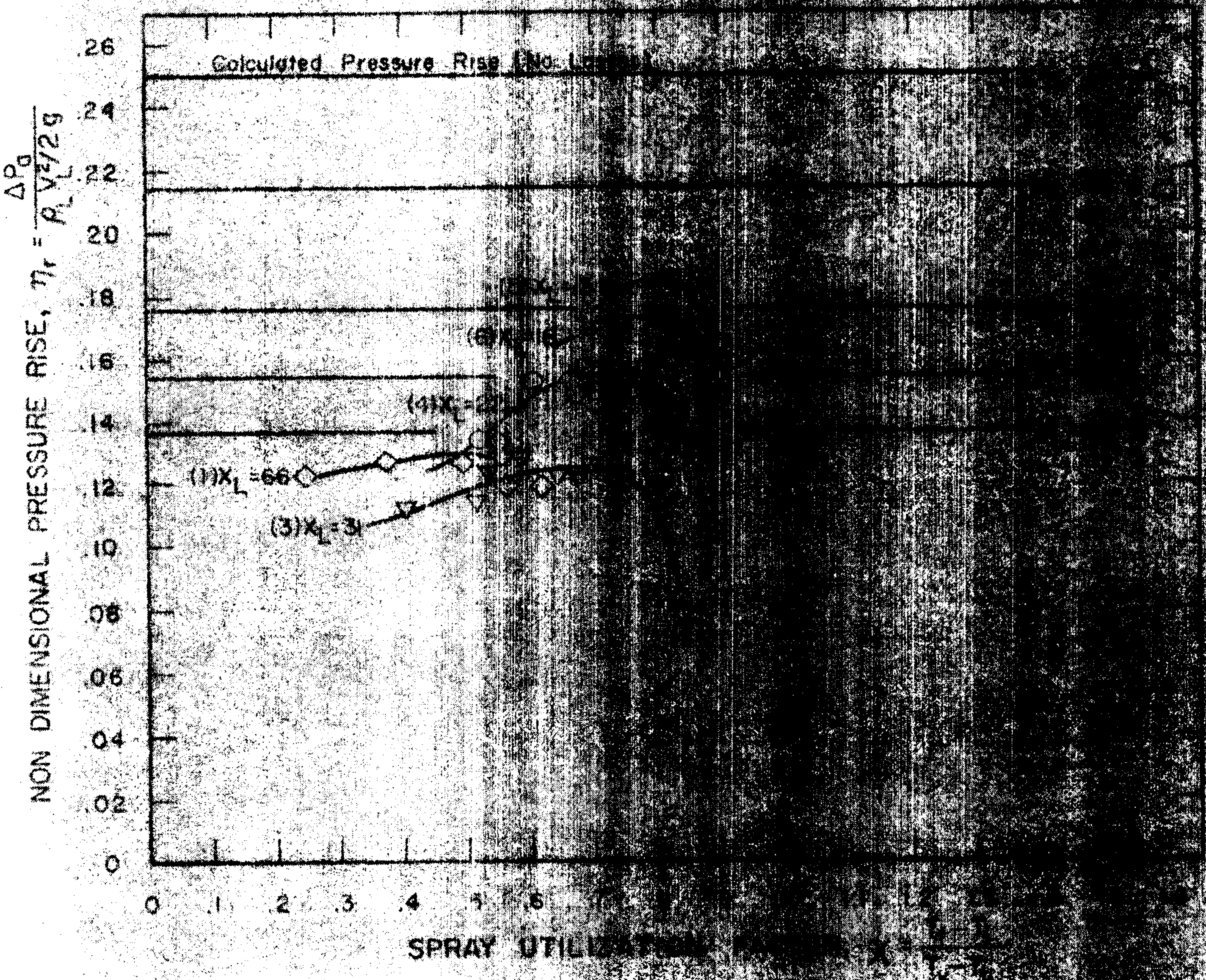

FIG. 4-3 NON-DIMENSIONAL PRESSURE [illegible] VS. [illegible] UTILIZATION [illegible] CONSTANT MASS FLOW RATIO) FOR [illegible] INJECTOR [illegible]

countered in space. [illegible]

[illegible] in the design of the [illegible] capacity of the boiler [illegible] increased in order to provide [illegible] liquid flow rates. A welded [illegible]

[illegible] test chamber. [illegible] from test sections can be eliminated, [illegible] similar to those encountered in space. Operation in the chamber is facilitated by:

1. Remote control of all valves.
2. A protective case around the loop to ensure that any mercury spills would not contaminate the environmental test chamber.
3. Loop assembly in a portable frame to allow easy removal from the test chamber and ready access for any repair work or modifications.
4. Use of vacuum seals for all electrical, water, and air leads going into the test loop.
5. Water cooling of the case in order to prevent excessive temperatures resulting from boiler and heater heat losses.

Fabrication and welding of the main flow circuit has been [illegible]

[illegible]

5.1 [illegible]

[illegible]

and flows through a [illegible] section of [illegible] tube diameters. This section is [illegible] in order to reduce heat loss. Pressure, temperature, and differential pressure measurements are taken at the test section. If spray condensing tests are being conducted, liquid is injected into the test section at the point of entrance of the vapor. The resulting condensate-liquid mixture flows out of the test section, bypasses the reservoir, and flows into a cooler where the liquid temperature is reduced to a value of 400°F, at which condition the flow enters the pump. The pump pressurizes the flow and returns a portion of it to the boiler while the rest flows through a heater and back into the test section. As can be seen from Fig. 5-3, flowmeters are provided for the boiler inlet, liquid injection, and calorimeter flows. Control of the flow is accomplished through pneumatically operated control valves as shown in Fig. 5-3.

TABLE 5-1

[illegible]

[illegible]	[illegible]
Vapor Pressure	4 - 10[illegible] psia
Quality	0 to 1.0
Vapor Flow Rate	0 to 270 lb/hr (600 lb/hr with slight mod.)
Heat Injection In Test Section	0 - 10 KW (2[illegible] KW with slight mod.)
[illegible]	[illegible]
Liquid Flow Rate	0 to 1[illegible] lb/hr ([illegible] psia)

[illegible]

One of the most valuable additions to instrumentation of the test [illegible]

[illegible] simple readout, and wide flow range.

In order to [illegible] the operation of these components, prelim- [illegible]

[illegible] means that testing can be conducted over wide ranges of flow rate with one flowmeter sensing element. In addition, the linear characteristic enables better estimates of flow rate to be made at higher flow rates (12,000 lbs/hr) where calibration becomes extremely difficult due to the large amount of mercury required.

5.2 Equipment

Boiler - The boiler has pool type construction with cartridge type heaters inserted into wells. All welded construction was utilized. The superheater is an integral part of the boiler and consists of a 1100 watt heater inserted into a well with an outside spiral flow passage.

The total number of boiler heater elements provided is 12 (1100 watts each). A baffle is provided at the vapor outlet in order to minimize liquid entrainment by the vapor.

[illegible]

trap which condenses any mercury vapor.

Cooler - The cooler was provided in order to lower the temperature of the liquid mercury to a value compatible with the pump and flowmeters. It consists of a coiled stainless steel tube (through which the mercury flows) surrounded by a brass case which is silver brazed on the main flow line. Water is circulated through the outer case. (All brass or copper parts are painted or coated in order to prevent corrosion from any mercury leaks.)

Pump - The pump used is a "Viking" all-stainless steel plain head pump with a Teflon mechanical seal. It is a constant speed gear pump. The rated capacity is 2 gpm at a pressure rise of 50 psid. A minor modification was made to the pump in order to allow use of liquid mercury at 400°F. The mechanical seal should

provide positive leak protection; however, the pump is located about

[redacted]

calibrations will be run on thermocouples before their use.

Differential Pressure Measurements - Differential pressure measurements are made with "Barton" bellows-type differential pressure gages. Readout is on a dial gage. In order to eliminate corrosion and buoyant problems chemical seals are used on two units. For the differential pressure gage across the injected liquid mercury (0 - 50 psid) a commercially available "Brooks" seal was used. However, the differential gage across the test section has a lower differential range (10 - 0 - 10 psid) and a much larger full scale displacement of the internal bellows in the gage. In order to provide a seal against the mercury for this gage, a chemical seal unit had to be designed and constructed using a flexible bellows to seal against the mercury and gage fill fluid. Quoted accuracies of the gages are ± 1/2 percent of the full scale reading.

<u>Pressure Gages</u> - The gages used for absolute measurements are "US Super Gages". These gages utilize stainless steel con- [illegible] The gages [illegible]

<u>Level Indicators</u> - The level indicator used on the boiler is a contact type. Lights are connected to a circuit which is closed when the liquid mercury closes contact between bare metal probes, giving a visual indication of the mercury level.

<u>Temperature Controller</u> - Temperature controller used on the boiler was a "Wheelco Capacitrol". The temperature controller is connected to one 1100 watt heating element in the boiler and is intended for use as a "fine" control device. Coarse control will be obtained through the use of off-on switches on the heating elements and a Variac.

<u>Flowmeters</u> - As discussed above, the flowmeters to be used are [illegible] with epoxy liners and probes which come in a direct contact with the liquid mercury. The readout instruments used are a Hewlett-Packard [illegible] and a [illegible] recorder.

<u>Photographic Instrumentation</u> - High speed photographs will be taken with a Fastax WF-3 camera which is capable of operation at 8000 frames/sec. Back lighting will be obtained with Sylvania "Tru-flector" type bulbs and a frosted glass piece to diffuse the light. A special fixture has been fabricated to enable use of the camera in the interior of the tank.

FIG. 5-1

10kw TEST LOOP CONTROL PANELS AND VIEWING PORT

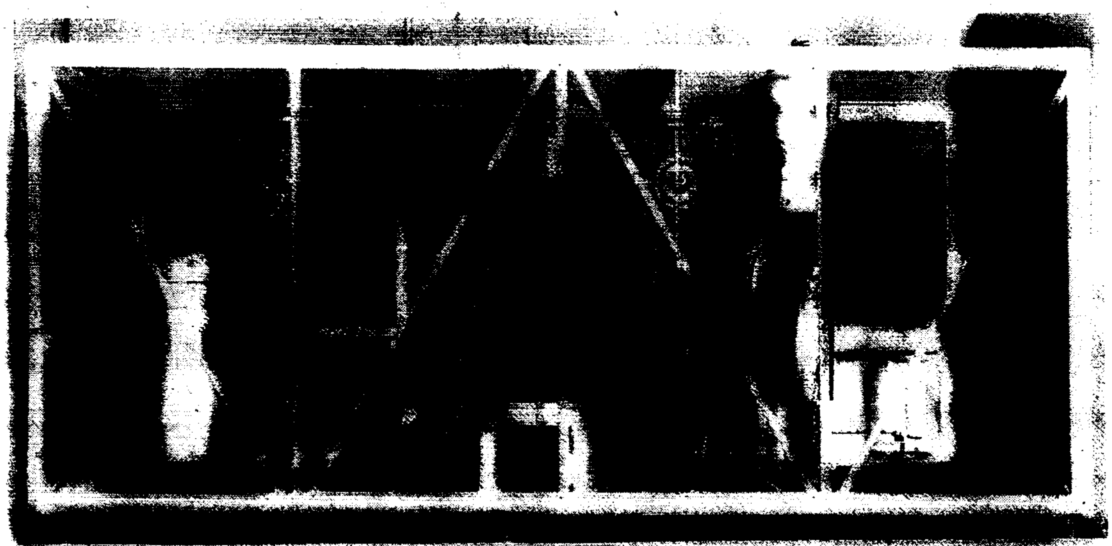

FIG. 5-2 10kw TEST LOOP MAIN FLOW CIRCUIT

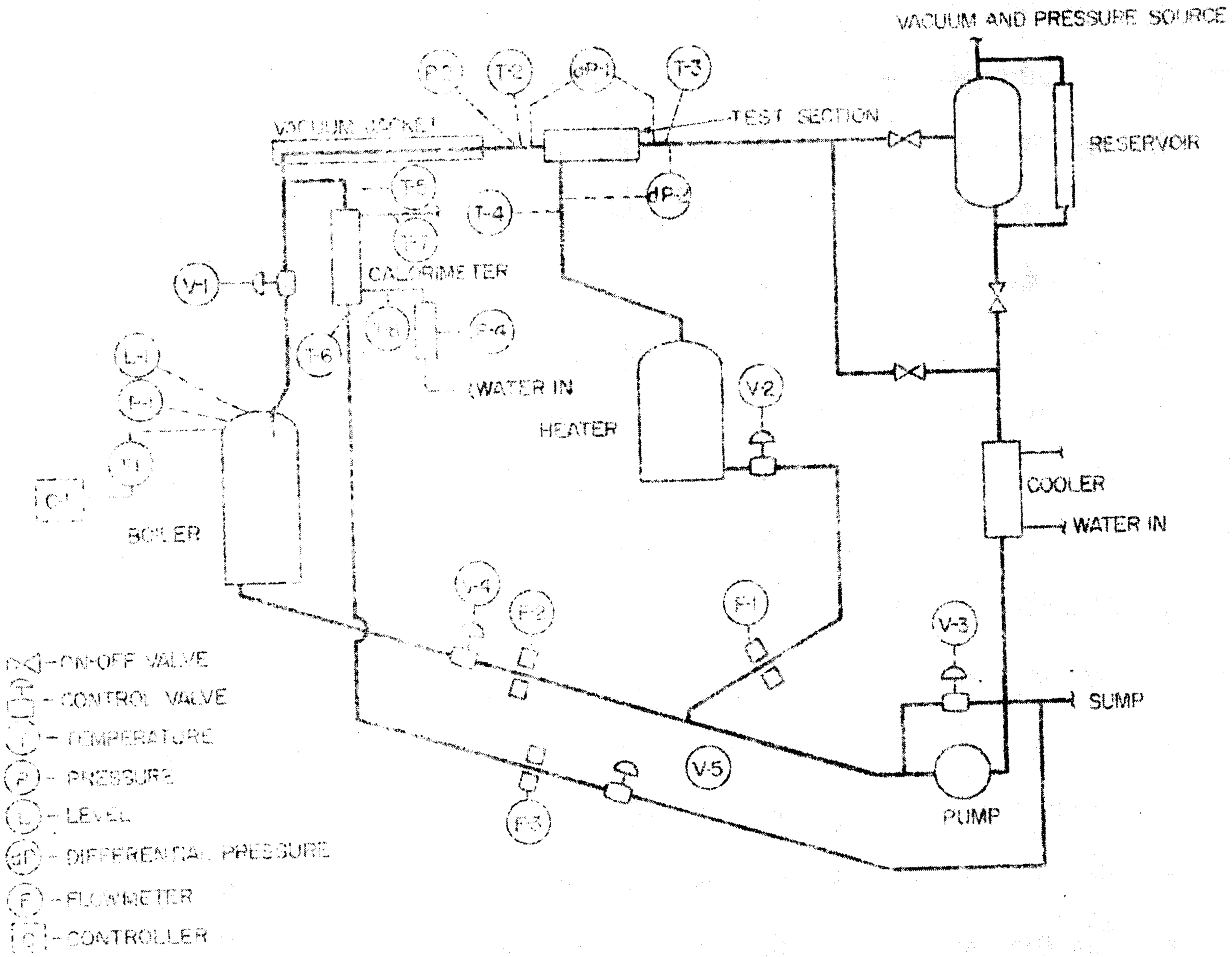

FIG. 5-3 10KW TEST LOOP SCHEMATIC

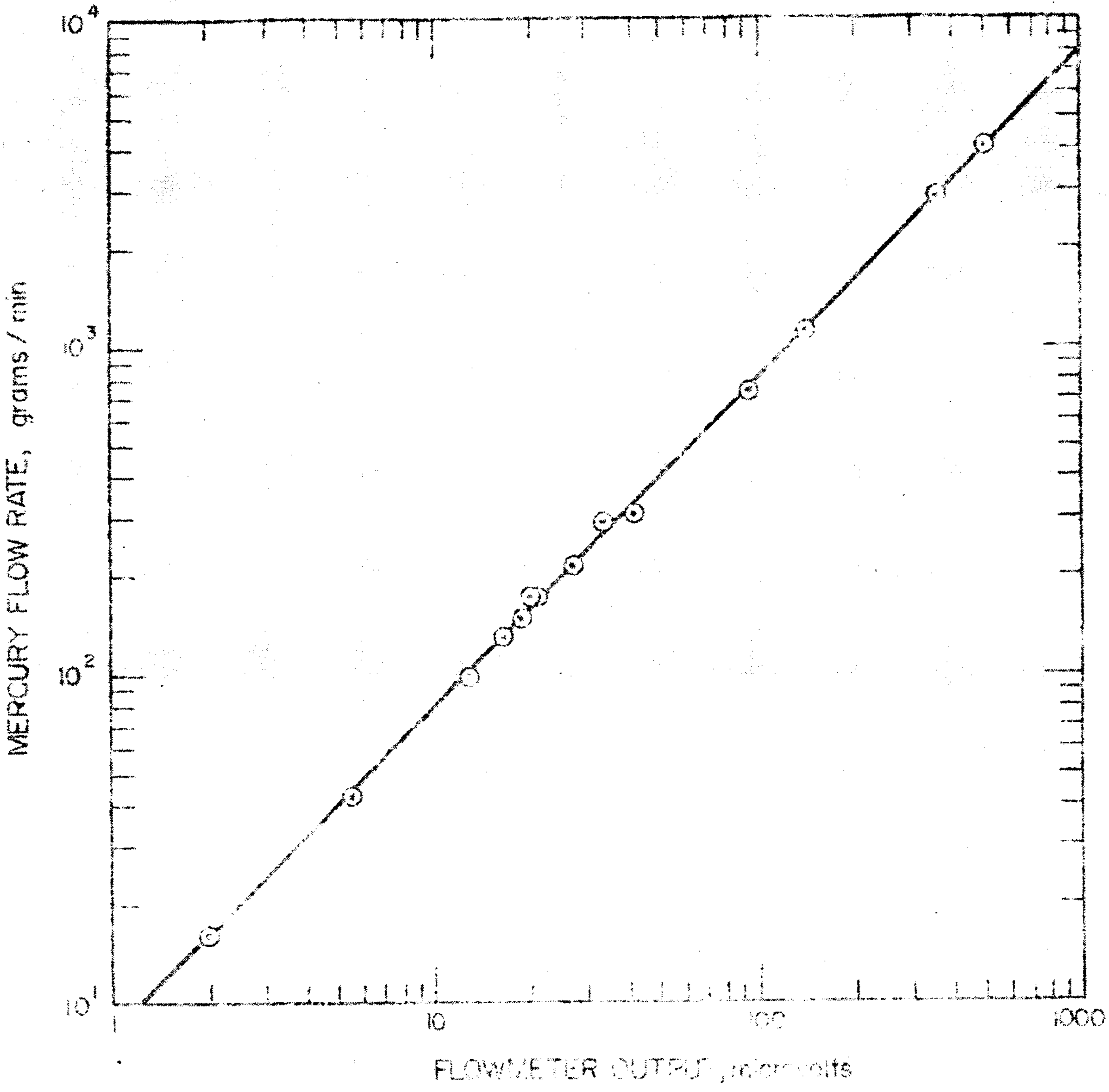

FIG. 5-4 PRELIMINARY CALIBRATION CURVE FOR BOILER INLET FLOW METER

REFERENCES

1. Electro-Optical Systems Report 500-F, Prepared for ABMA under Contract DA-04-495-506-ORD-2007, L. Hays, "Condenser Space Heat Rejection Systems", 19 December 1960, Pasadena, California

2. Proceedings of NASA sponsored Government-Industry Meeting on Mercury Condensing; Chairman, S. Lieblein, NASA Lewis Research Center, 18 April 1961, Held at Electro-Optical Systems, Inc, Pasadena, California

3. M. G. Coombs, R. A. Stone, I. Kapus. Atomics International, "The SNAP 2 Radiative Condenser Analysis", Report NAA-SR-5317, Prepared under Contract AT(11-1)-Gen-8 for the AEC.

4. R. C. Martinelli and D. B. Nelson, "Prediction of Pressure Drop During Forced-Circulation Boiling of Water", ASME Annual Meeting, December 1947.

5. R. W. Lockhart and R. C. Martinelli, "Proposed Correlation of Data for Isothermal Two-Phase, Two Component Flow in Pipes". Chem. Engr. Prog. Vol. 45 No. 1, January 1949.

6. Electro-Optical Systems Report 1588-ML-5, Prepared for NASA under Contract NAS 7-11, "Condenser Heat Rejection Systems" 7 April 1961, Pasadena, California